

# **Amine or Azo Functionalized Hypercrosslinked Polymers for Highly Efficient CO<sub>2</sub> Capture and Selective CO<sub>2</sub> Capture**

Yuanting Qiao,<sup>a</sup> Zhen Zhan,<sup>b</sup> Yuwan Yang,<sup>b</sup> Manying Liu,<sup>c</sup> Qi Huang,<sup>a</sup> Bien Tan,<sup>b</sup> Xuebin Ke,<sup>d</sup> Chunfei Wu<sup>a\*</sup>

a. School of Chemistry and Chemical Engineering, Queen's University Belfast, Belfast, UK BT7 1NN.

b. Key Laboratory of Material Chemistry for Energy Conversion and Storage, Ministry of Education, School of Chemistry and Chemical Engineering, Huazhong University of Science and Technology, Luoyu Road No. 1037, 430074 Wuhan, China.

c. Key Laboratory of Micro-Nano Materials for Energy Storage and Conversion of Henan Province, Institute of Surface Micro and Nano Materials, College of Chemical and Materials Engineering, Xuchang University, Henan 461000, P. R. China

d. Department of Chemical Engineering, University of Hull, Hull, UK, HU6 7RX.

Corresponding author: Dr Chunfei Wu (c.wu@qub.ac.uk)

## **Abstract**

**Hypercrosslinked polymers (HCPs) are very promising for large-scale application due to their easy preparation, high thermal stability and good capability of CO<sub>2</sub> capture. Currently many amine-functionalized porous materials were prepared through two steps, but in this paper the amine-functionalized HCPs was obtained with one-step method and it showed high CO<sub>2</sub> adsorption up to 4.24 mmol/g at 273 K. In addition, since the azo-functionalized porous materials have many potential applications including supports for noble metal catalysts and the photoresponsive 'smart' materials, azobenzene are attracting functional groups for the porous materials. In this paper the azo-functionalized HCPs is firstly reported, and it is used as CO<sub>2</sub> adsorbents (3.02 mmol/g at 273 K) performing good CO<sub>2</sub>/N<sub>2</sub> selectivity (34.52 at 298 K).**

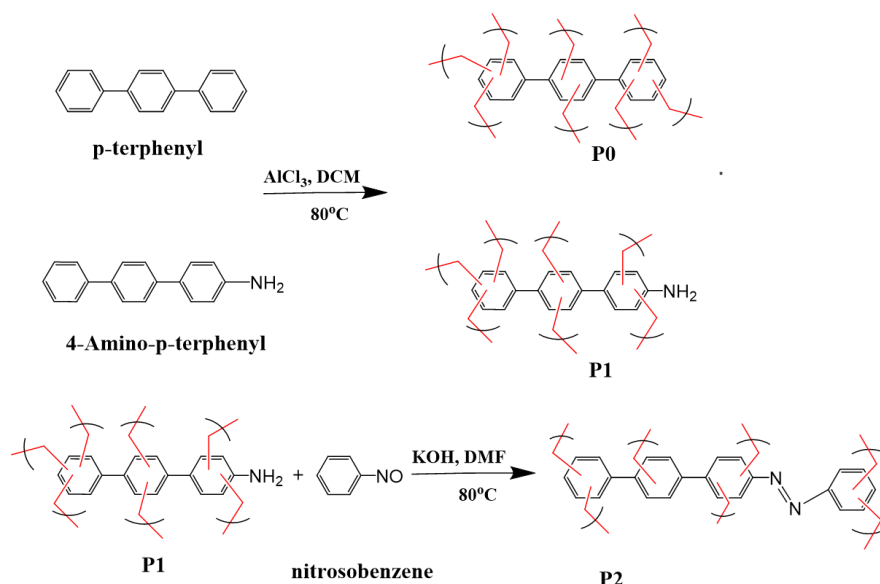
## **KEYWORDS**

Hypercrosslinked polymers (HCPs), amine, azobenzene, CO<sub>2</sub> adsorption, CO<sub>2</sub>/N<sub>2</sub> selectivity

## 1. Introduction

The concentrations of CO<sub>2</sub> in the atmosphere has increased to their highest level ever, at 408 parts per million—about 45 percent higher than their preindustrial levels.<sup>1</sup> As the excess amount of CO<sub>2</sub> is the most relevant contributor to climate change, it is desiring to develop efficient sorbents to capture CO<sub>2</sub>.<sup>2-3</sup> Different methods including absorption, adsorption, membrane separation, or cryogenic distillation processes have been researched to capture CO<sub>2</sub>.<sup>4-6</sup> Among them, adsorption is proposed as one promising way to capture CO<sub>2</sub> because of its high adsorption capacity, easy regeneration and strong stability. Aqueous amine, as a commonly used adsorbent of CO<sub>2</sub> in industry, has distinct disadvantages such as high regeneration costs, volatility, and corrosion of the equipment.<sup>7-8</sup> Thus, using porous organic polymers (POPs) including covalent organic frameworks (COFs),<sup>9-10</sup> hypercrosslinked polymers (HCPs),<sup>11-12</sup> conjugated microporous polymers (CMPs),<sup>13-14</sup> polymers of intrinsic microporosity (PIM),<sup>15</sup> covalent triazine frameworks (CTFs),<sup>16-18</sup> and porous aromatic frameworks (PAFs),<sup>19</sup> have been researched intensively because they usually perform good capacity of capture CO<sub>2</sub> with low-energy regeneration.<sup>20-21</sup> Compared with other organic porous materials, HCPs are very promising for large-scale application due to their remarkable advantages, such as low cost, easy large scale application, easy functionalization, high surface area, excellent chemical and thermal stability and mild operating conditions.<sup>11-12</sup> To obtain the HCPs with excellent CO<sub>2</sub> uptake capacity under the simple synthesis conditions, Tan's group developed the solvent knitting method through a simple one-step Friedel-Crafts alkylation reaction with the use of dichloroalkane as an economical solvent, stable electrophilic reagent, and external cross-linker.<sup>22-23</sup>

To increase the capacity of CO<sub>2</sub> capture and the selectivity, the introduction of basic nitrogen functionalities, such as amine,<sup>24</sup> amide,<sup>25</sup> azobenzene,<sup>26-28</sup> triazine,<sup>29-30</sup> carbazole,<sup>31</sup> porphyrin units,<sup>32</sup> and naphthyl groups<sup>33</sup> into porous materials, has been proven to be beneficial for gas storage due to the activation of CO<sub>2</sub> from their CO<sub>2</sub>-philic nature.<sup>34-35</sup> Among them, the azo functional groups are very attracting, because they are also highly selective and sensitive toward the incorporation of various metal ions and are thought as potential candidate of heterogeneous supports for noble metal catalysts.<sup>26</sup> The photoresponsive nature of azobenzene and its derivatives also make the azo-functionalized porous materials possible candidates as stimuli-responsive 'smart' materials.<sup>27, 36-39</sup> However, most of the functionalized HCPs were synthesized through rigorous conditions, multi-steps, using the expensive catalysts, with low amine content,



**Scheme 1.** Synthetic schematic diagram of P0, P1 and P2.

low thermal stability. For example, Turner et al.<sup>24</sup> developed series of amine-containing HCPs-based  $\text{CO}_2$  adsorbents, divinylbenzene-maleic anhydride (DVB-MAH) copolymer with various diamines, through a two-step post-modification. The HCPs showed low  $\text{CO}_2$  capture capacity (0.96-1.53 mmol/g at 273 K and 1 bar). Recently, Liu et al.<sup>40</sup> also reported one type of amine-functionalized HCPs (XAD-4-pc) through two steps including the reaction of Friedel-Crafts, and impregnation with polyethyleneimine (PEI) for  $\text{CO}_2$  capture with the reaction temperature around 350-500°C. The maximum  $\text{CO}_2$  uptake for PEI-functionalized XAD-4-pc was 3.24 mmol  $\text{g}^{-1}$  at 298K, but the reaction temperature will lead to high cost. Though such progress has been made, it is still desirable to develop a simple and efficient route for the production of reported amine/azo-functionalized POPs under mild and easy handling conditions with good  $\text{CO}_2$  capture capacities and selectivity.

Herein, we synthesized amine/azo functionalized HCPs under the simple synthesis conditions, respectively. HCPs are very stable with excellent  $\text{CO}_2$  uptake capacity and good  $\text{CO}_2/\text{N}_2$  selectivity. To our best knowledge, the azobenzene functional group is introduced into HCPs firstly, which can be used to other application in the future. The amine-functionalized HCPs was synthesized using the Friedel-Crafts alkylation reaction of 4-Amino-p-terphenyl with dichloromethane (DCM as solvent and cross-linker) in the presence of  $\text{AlCl}_3$  catalyst (Scheme 1, defined as P1). Then azo-functionalised HCPs (Scheme 1, P2) was prepared by the polymerization of P1 and nitrosobenzene due to the fact that nitrosobenzene and aniline could react to form azobenzene.<sup>41</sup> In addition, P0, without any functional group, was synthesized from p-terphenyl and DCM under the same condition, with same monomer ratio for comparison (Scheme 1).

## 2. Experimental Materials and methods

### 2.1 Chemicals.

All reagents were used as purchased without further purification. P-terphenyl and 4-Amino-p-terphenyl were purchased from Aladdin chemical reagent Corp (Shanghai, China). DCM, ethanol, nitrobenzene, HCl, and anhydrous aluminum chloride were obtained from Sinopharm chemical reagent Co., Ltd (Shanghai, China).

### 2.2 Materials Synthesis.

**Synthesis of P0** Under N<sub>2</sub> atmosphere, p-terphenyl (1 mmol 0.230g) was dissolved in DCM (8 mL), and then the catalyst (AlCl<sub>3</sub>, 12 mmol, 0.399g) was added at room temperature. The reaction system was then stirred at 0 for 4 h, 30°C for 8h, 40 °C for 12 h, 60°C for 12 h and 80 °C for 24 h to obtain the polymer. The resulting solid was quenched using 20 ml of HCl-H<sub>2</sub>O (v/v=2: 1), and washed twice with water and twice with ethanol, followed by further purification by extracting with ethanol for 48 h. Finally, the solid was dried in a vacuum oven at 65 °C for 24 h.

**Synthesis of P1** P1 was obtained using the same procedure of P0 with the monomer 4-Amino-p-terphenyl (1 mmol 0.245g) dissolved in DCM (8 mL), and the catalyst (AlCl<sub>3</sub>, 12 mmol, 0.399g). The reaction system was heating from 0°C to 80 °C following the same route mentioned above in synthesis of P0. The resulting solid was quenched using 20 ml of HCl-H<sub>2</sub>O (v/v=2: 1), and ethanol separately. Finally, the solid was dried in a vacuum oven at 65 °C for 24 h.

**Synthesis of P2** The reaction of nitrobenzene (1 equivalent) and P1 (3 equiv) in DMF (5 mL), under N<sub>2</sub> for 12 h afforded P2.

### 2.3 Characterization

The obtained samples were characterized in terms of chemical composition and surface chemistry to detect and verify the existence of surface functional groups. Solid state <sup>13</sup>C cross-polarization/magic-angle spinning nuclear magnetic resonance (<sup>13</sup>C CP/MAS NMR) spectra were recorded on a WB 400 MHz Bruker Avance III spectrometer and collected with a spinning rate of 20 kHz by using a 2.5 mm double-resonance MAS probe. The samples were determined using a Bruker VERTEX 70 Fourier-transform infrared spectroscopy (FTIR) machine to obtain spectrum in the range of 500-4000 cm<sup>-1</sup>. Element analysis was carried out using a CHNS Elemental Analyzer (Perkin Elmer PE2400CHNS) in order to determine the chemical composition of the samples. The field-emission scanning electron microscopy (FE-SEM) images were recorded on a FEI Quanta FEG - Environmental SEM Oxford Ex-ACT analyzer operating at 10 kV.

Thermogravimetric analysis (TGA) was performed from room temperature to 850 °C, using a Mettler Toledo DSC / TGA 1 Star TGA with a heating rate of 10 °C min<sup>-1</sup> under a nitrogen atmosphere. The surface area and pore size were investigated using a Micromeritics ASAP 2020 M analyzer. All samples were vacuum degassed at 150 °C overnight to remove volatiles and used for characterization. Nitrogen adsorption-desorption isotherms were obtained at 77 K and a partial pressure range of (0.005–0.99), adsorption-desorption isotherms were further used for estimation of BET surface area, pore volume, and pore size distribution. BET surface area was calculated using multi-point test in a partial pressure range of (0.05–0.3), micropore volume was estimated using Non-Local Density Functional Theory (NDLFT). Total pore volume was measured at a partial pressure of 0.99. Mesopore volume was calculated as the difference of total pore volume at 0.99 and micropore volume. Gas (CO<sub>2</sub> and N<sub>2</sub>) adsorption and desorption isotherms were measured on a Micromeritics ASAP 2020 M analyzer at 273.15 K. CO<sub>2</sub>/N<sub>2</sub> selectivity is calculated at 298 K using initial slope method.

### 3. Results and discussion

#### 3.1 Polymer characterisation

The molecular structure of the HCPs was characterized using CP-MAS <sup>13</sup>C NMR spectra (Figure 1. a). The resonance peaks around 130 ppm and 139 ppm are due to nonsubstituted aromatic carbon and substituted aromatic carbon, respectively, and the resonance peaks near 35 ppm and 18 ppm are due to carbon in methylene linker formed after Friedel-Crafts reaction, while the amine bond is not obvious. The similar results are also reported.<sup>22, 42-43</sup>

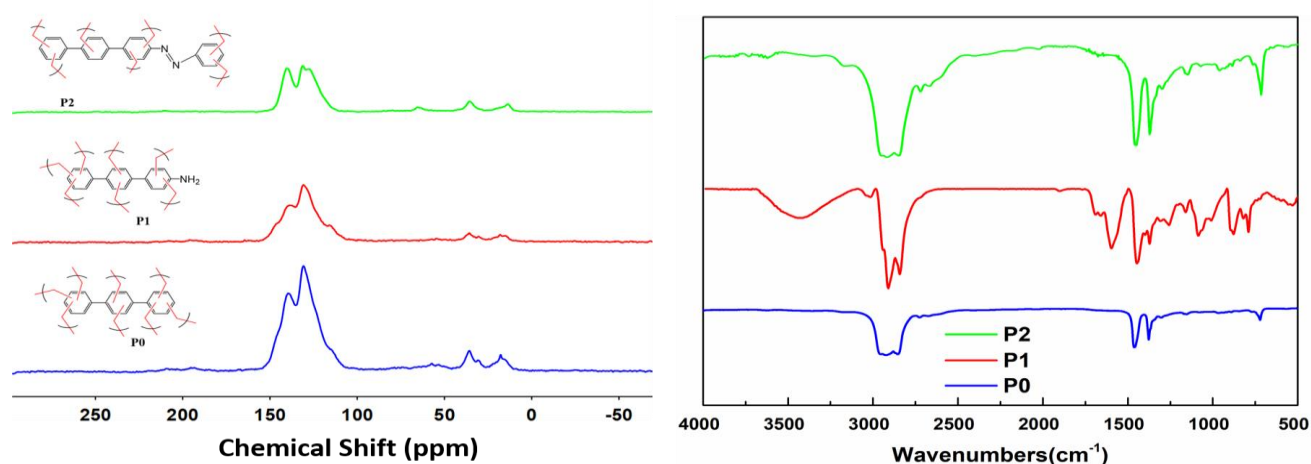


**Figure 1.** (a) Solid state cross-polarization (CP)<sup>13</sup>C MAS NMR of P0, P1 and P2. P0 was obtained from the monomer of p-terphenyl, while P1 was from p-terphenyl. P2 was prepared with the azo functional group. (b) FT-IR spectra results of P0, P1 and P2.

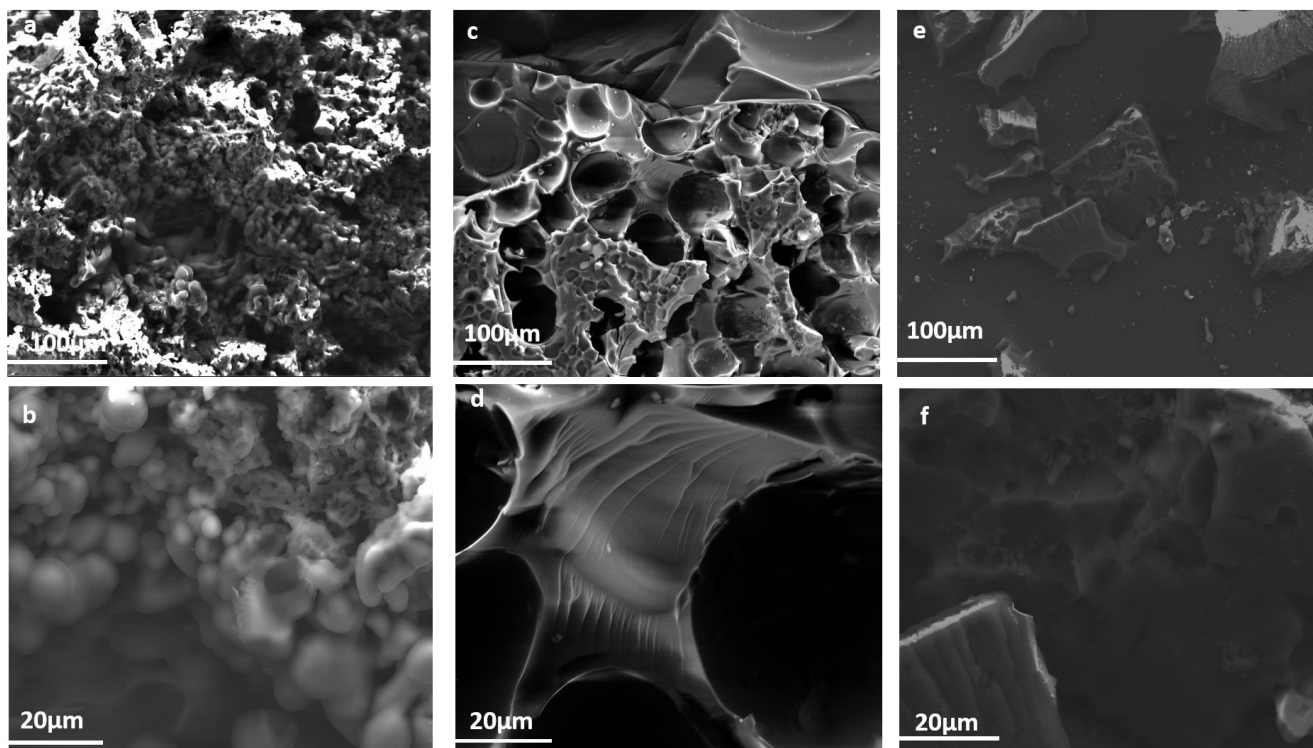


**Figure 2.** SEM images for P0 (a and b), P1 (c and d) and P2 (e and f) with a scale bar of 100  $\mu\text{m}$  and 20  $\mu\text{m}$ , respectively.

In the FTIR spectra results, the peaks around  $1450\text{ cm}^{-1}$  and  $2900\text{ cm}^{-1}$  in three polymers are related to the C=C stretching vibrations and C-H stretching vibrations of methylene, respectively, proving the successful synthesis of HCPs.<sup>22</sup> Moreover, the peaks at  $3438\text{ cm}^{-1}$ ,  $1598\text{ cm}^{-1}$ ,  $883\text{ cm}^{-1}$  and  $1265\text{ cm}^{-1}$  in the FTIR spectrum are associated with the N-H stretching, N-H bending, N-H wagging vibrations and C-N stretch inside P1, respectively, which confirm the existence of amine (Figure 1. b).<sup>29, 44-45</sup> In addition, the peaks of  $1305\text{ cm}^{-1}$  is responding to the N=N stretching band in P2, indicating the azobenzene group is stable and retained in the frameworks.<sup>26-27</sup> Furthermore, the nitrogen content was also tested by elemental analysis. P2 was found to contain 5.88% N, which is higher than that of P0 (<0.3%) and P1 (3.89%). P2 contains the largest quantity of N, because of the N=N bond in the azo group.

In addition, these polymers exhibit high thermal stability confirmed by the result of the TGA test. Both polymers retain more than 60% of their mass even at  $800\text{ }^{\circ}\text{C}$  (Figure S1). We further investigated the morphology of polymers by FE-SEM as shown in Figure 2. The morphology of P0 (Figure 2 a and b) shows the aggregations of uniform particles, while that of P1 and P2 demonstrates pores (Figure 2 c and d). The similar structure has been reported previously.<sup>22</sup>

The porosity properties of the polymers were further investigated by  $\text{N}_2$  adsorption measured at 77K (Figure 3. a) and the pore characteristics of all samples are summarized in Table 1. P0, P1 and P2 are microporous materials because they exhibit type I isotherms, where the uptake of  $\text{N}_2$

sharply climbs in the low relative pressure's region ( $P/P_0 < 0.001$ ), and almost reaches a plateau at higher pressure. The existence of the hysteresis loops in desorption isotherms of P0 (Figure 3. a) proves the presence of mesopores, which is consistent with the result of pore size distributions of P0 calculated by using NLDFT (Figure 3 b). P0 exhibits apparent peaks located primarily in the micropore region and continuous mesopores ranging from 2 nm to 5 nm. P2 have the narrowest pore size distribution shown in the Fig. 3 b, while in terms of P1, most peaks stay in the micropore region ( $< 2$  nm) ranging from 1.6 nm to 1.8 nm. All polymers show hierarchical pores with ultra-micropores (less than 0.7 nm). In addition, the average pore diameter of P1 and P2 are similar, with 1.91nm and 1.94nm respectively, and they are smaller than that of P0 (5.65 nm) significantly (table 1). The smaller pore size is very important for CO<sub>2</sub> adsorption, because smaller pore size results in deep overlap of potential and thus strong interaction.<sup>16, 46-47</sup> The BET surface areas and pore volume of P0 are the largest, with 1062.19 m<sup>2</sup>/g and 0.69 cm<sup>3</sup>/g, respectively. The reason that the surface area and pore volume of P1 and P2 are less than P0 may be the occupation of the pore channels by the amine group, which has also been confirmed by similar research.<sup>40</sup>

### 3.2. CO<sub>2</sub> Adsorption Properties

According to the demand of the technology to capture the CO<sub>2</sub> capture, HCPs is regarded as one efficient CO<sub>2</sub> adsorbent because of its low cost, easy preparation and good sorption property. The CO<sub>2</sub> adsorption isotherms were investigated at 273 K up to 1.1 bar (Figure 3. c). P1 shows remarkable uptake of CO<sub>2</sub> up to 4.24 mmol/g (18.7 wt%) at 273 K, 1.13 bar, which is better than P0 and P2. It should be attributed to the presence of the amine group in P1, because amine groups offer the CO<sub>2</sub>-philic site, which can greatly promote the physicochemical affinity between the polymers and CO<sub>2</sub> molecule.<sup>25, 34-35, 45, 48</sup> In addition, P1 was compared with many previously reported porous materials with nitrogen

**Table 1.** Porous Texture Properties of P0, P1 and P2.

Sample	S <sub>BET</sub> <sup>a</sup> (m <sup>2</sup> /g)	V <sub>t</sub> <sup>b</sup> (cm <sup>3</sup> /g)	V <sub>0.1</sub> <sup>c</sup> (cm <sup>3</sup> /g)	PD <sup>d</sup> (nm)	CO <sub>2</sub> uptake <sup>e</sup> (mmol/g)	CO <sub>2</sub> /N <sub>2</sub> selectivity <sup>f</sup>
P0	1062	0.69	0.28	5.65	3.79	18.28
P1	447	0.21	0.16	1.91	4.24	20.97
P2	242	0.12	0.09	1.94	3.02	34.52

<sup>a</sup> Apparent surface area was calculated using the BET method at 77K. <sup>b</sup> Total pore volume calculated from the nitrogen isotherm at  $P/P_0 = 0.99$  and 77.3 K. <sup>c</sup> Micropore volume using the t-plot method at  $P/P_0 = 0.050$ . <sup>d</sup> Average pore diameter. <sup>e</sup> Measured at a pressure of 1 bar using a Micromeritics ASAP 2020 M analyzer at 273.15 K. <sup>f</sup> CO<sub>2</sub>/N<sub>2</sub> selectivity is calculated at 298 K using initial slope method.

containing groups and the results are summarized in Table 2. Its capacity of CO<sub>2</sub> adsorption is also higher than them. With the good capacity of CO<sub>2</sub> uptake and easy preparation procedure, P1 is of high potential for the capture of CO<sub>2</sub>.

Though uptake of CO<sub>2</sub> of P2 is the lowest (3.02 mmol/g at 273 K, 1.13 bar), because the BET surface areas and pore volume of P2 are the lowest. On the other hand, the CO<sub>2</sub>/N<sub>2</sub> selectivity for P2 was calculated to be 34.52 at 298 K, which is highest among these three polymers (Table 1 and Figure S2). This difference is mainly because azo-containing sites in P2 contribute to the CO<sub>2</sub> adsorption, but perform N<sub>2</sub> phobicity. This nature has been also used by Hasmukh A. Patel, to prepare high-temperature (>40 °C) CO<sub>2</sub> selectivity in N<sub>2</sub>-phobic nanoporous covalent organic polymers.<sup>49</sup> As a good selectivity of CO<sub>2</sub> over N<sub>2</sub> is also important for industrial application of CO<sub>2</sub> adsorbent, P2 is also promising candidate

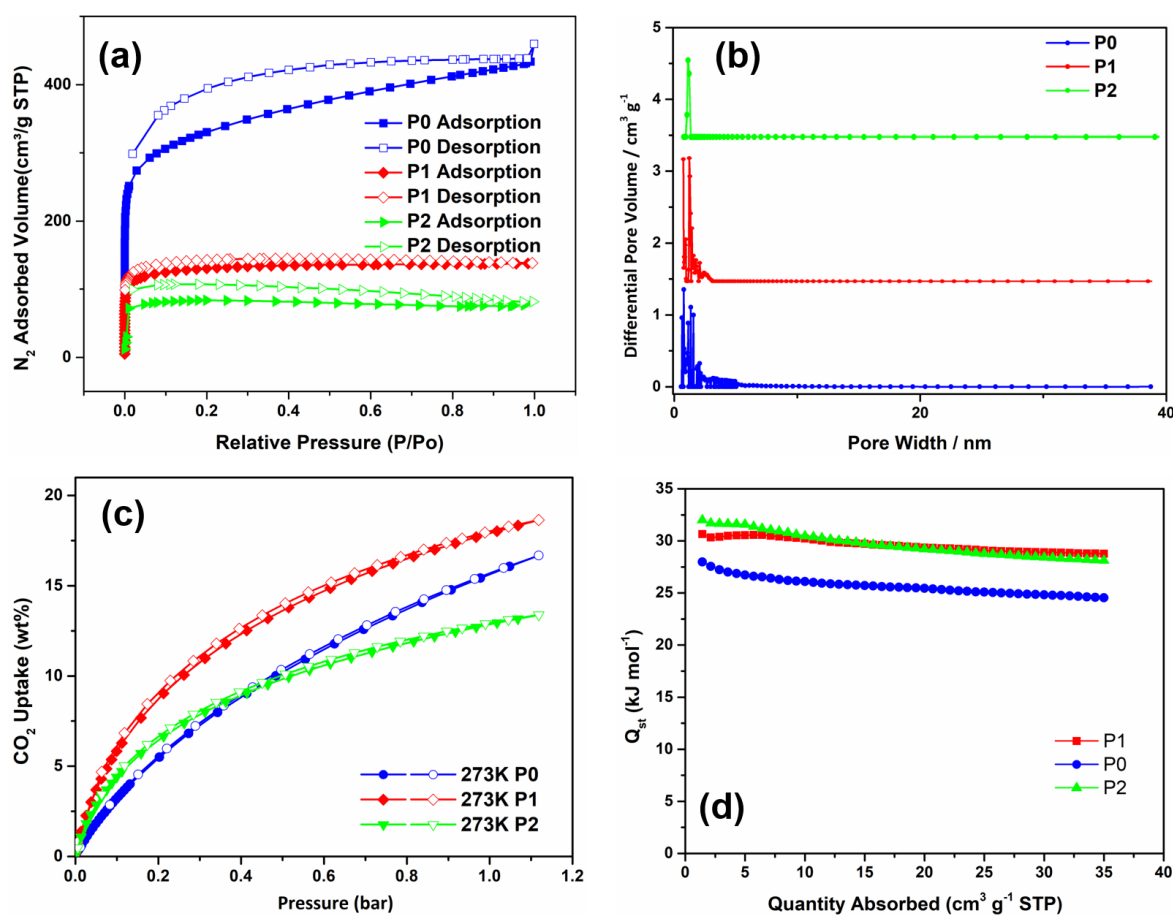


**Figure 3.** (a) Nitrogen adsorption and desorption isotherms of P0 (up) and P1 (bottom) measured at 77.3 K and 1.00 bar. Open symbols represent adsorption and filled symbols represent desorption. (b) Pore size distribution curves of P0 (up) and P1 (bottom) calculated using nonlocal density functional theory (slit pore models, differential pore volumes, pore width). (c) Volumetric CO<sub>2</sub> adsorption isotherms and desorption isotherms of P0 and P1 up to 1.13 bar at 273.15 K. Open symbols represent adsorption and filled symbols represent desorption. (d) Isothermic heat of adsorption calculated at different CO<sub>2</sub> loadings.

for CO<sub>2</sub> adsorbents.

To confirm the relationship between polymer networks and CO<sub>2</sub> molecules, the isosteric heat ( $Q_{st}$ ) of adsorption for the materials was calculated by fitting the CO<sub>2</sub> adsorption isotherms collected at 273.15 and 298.15 K according to the Clausius–Clapeyron equation (Figure 3. d ).<sup>33</sup> For all samples,  $Q_{st}$  are in the range between 24 and 32 kJ/mol in the loading range of CO<sub>2</sub> between 1.43 and 27.98 m<sup>3</sup>/g, which are higher than 20 kJ mol<sup>-1</sup>, although not yet in the well-defined region of chemisorption ( $Q_{st} > 40$  kJ mol<sup>-1</sup>),<sup>50</sup> thus confirming the combined nature (both physical and chemical of the CO<sub>2</sub> adsorption).<sup>51</sup> The values of  $Q_{st}$  decreases with the increase of adsorption amount of CO<sub>2</sub> because most of adsorption sites are occupied by CO<sub>2</sub> at the beginning, resulting in the decreasing trend of adsorption heat at higher adsorption amount<sup>40</sup>.  $Q_{st}$  of P1 and P2 are very similar, and are obviously higher than P0, which might be attributed to the amine/azo groups for the better affinity towards CO<sub>2</sub>. In addition, the introduction of nitrogen atoms to the networks is reported to improve the isosteric heat of ideal polymer materials, P1 and P2 performed higher isosteric heat than similar polymers reported.<sup>33</sup>

**Table 2.** Summary of surface area and CO<sub>2</sub> uptake at 273 K, 1 bar in nitrogen-doped functionalized porous materials.

T (K) =	Surface area (m <sup>2</sup> /g)	CO <sub>2</sub> uptake (mmol g <sup>-1</sup> )	Ref.
P1	447	3.65	This work
XAD-4-pc	1239	-	40
Azo-POF-1	712	2.98	28
Azo-POF-2	439	1.92	
Azo-MOP-1	456	2.21	
Azo-MOP-2	706	3.06	26
Azo-MOP-3	523	1.85	
Azo-MOP-4	335	1.77	
Azo-PPor-1	750	2.45	
Azo-PPor-2	664	2.23	32
Azo-PPor-3	587	2.26	
CTF-FUM-350	230	3.49	
CTF-FUM-400	480	2.45	
CTF-FUM-500	603	2.40	16
CTF-DCN-400	690	2.12	
CTF-DCN-500	735	2.69	
CMP-1-NH <sub>2</sub>	710	-	48

PAF-32-NH <sub>2</sub>	1230	-	52
PAF-33-NH <sub>2</sub>	370	1.19	53
NPOF-4-NH <sub>2</sub>	554	-	44
HCP-A	412	1.21	
HCP-B	500	1.46	
HCP-C	346	1.15	24
HCP-D	343	1.53	
HCP-E	183	0.96	

## Conclusions

In summary, we have successfully synthesized new amine/azo-functionalized porous materials, P1 and P2, by introducing -NH<sub>2</sub>/azo groups into HCPs. These polymers are tested to perform very thermally stable. P1, amine-functionalized HCPs, shows good CO<sub>2</sub> adsorption capacities up to 4.24 mmol/g at 273 K, while P2, azo-functionalized HCPs, shows a higher CO<sub>2</sub>/N<sub>2</sub> selectivity (34.52). Although, very similar polymers without functionalities, P0, show higher BET surface area and pore volumes, but P1 and P2 exhibit better CO<sub>2</sub> adsorption capacities and CO<sub>2</sub>/N<sub>2</sub> selectivity than P0. The reason is supposed to be the combined effect of the N-containing sites and pore size. More importantly, when P1 is compared with many other CO<sub>2</sub> adsorbents reported, it shows better capability of CO<sub>2</sub>. Some of them are prepared through two-step method of post modification, while P1 is obtained by one-step method. These results show that designing porous materials with amine/azo groups is a useful strategy for CO<sub>2</sub> capture.

## ACKNOWLEDGMENT

The authors gratefully acknowledge financial support from the China Scholarship Council (student number 201706880031). This project has received funding from the European Union's Horizon 2020 research and innovation programme under the Marie Skłodowska-Curie grant agreement No 823745.

## ABBREVIATIONS

Azo, azobenzene; HCPs, Hypercrosslinked polymers.

## REFERENCES

1. Atmospheric greenhouse gas concentrations. <https://www.eea.europa.eu/data-and-maps/indicators/atmospheric-greenhouse-gas-concentrations-6/assessment-1>.

2. Samanta, A.; Zhao, A.; Shimizu, G. K.; Sarkar, P.; Gupta, R., Post-combustion CO<sub>2</sub> capture using solid sorbents: a review. *Industrial & Engineering Chemistry Research* **2011**, *51* (4), 1438-1463.
3. Yu, K. M. K.; Curcic, I.; Gabriel, J.; Tsang, S. C. E., Recent advances in CO<sub>2</sub> capture and utilization. *ChemSusChem: Chemistry & Sustainability Energy & Materials* **2008**, *1* (11), 893-899.
4. Yu, C.-H.; Huang, C.-H.; Tan, C.-S., A review of CO<sub>2</sub> capture by absorption and adsorption. *Aerosol Air Qual. Res* **2012**, *12* (5), 745-769.
5. Wang, M.; Joel, A. S.; Ramshaw, C.; Eimer, D.; Musa, N. M., Process intensification for post-combustion CO<sub>2</sub> capture with chemical absorption: A critical review. *Applied Energy* **2015**, *158*, 275-291.
6. Giordano, L.; Gubis, J.; Bierman, G.; Kapteijn, F., Conceptual design of membrane-based pre-combustion CO<sub>2</sub> capture process: Role of permeance and selectivity on performance and costs. *Journal of membrane science* **2019**, *575*, 229-241.
7. Oyenekan, B. A.; Rochelle, G. T., Alternative stripper configurations for CO<sub>2</sub> capture by aqueous amines. *AIChE Journal* **2007**, *53* (12), 3144-3154.
8. Dave, N.; Do, T.; Puxty, G.; Rowland, R.; Feron, P.; Attalla, M., CO<sub>2</sub> capture by aqueous amines and aqueous ammonia—A Comparison. *Energy Procedia* **2009**, *1* (1), 949-954.
9. Feng, X.; Ding, X.; Jiang, D., Covalent organic frameworks. *Chemical Society Reviews* **2012**, *41* (18), 6010-6022.
10. Cote, A. P.; Benin, A. I.; Ockwig, N. W.; O'keeffe, M.; Matzger, A. J.; Yaghi, O. M., Porous, crystalline, covalent organic frameworks. *science* **2005**, *310* (5751), 1166-1170.
11. Huang, J.; Turner, S. R., Hypercrosslinked polymers: a review. *Polymer Reviews* **2018**, *58* (1), 1-41.
12. Tan, L.; Tan, B., Hypercrosslinked porous polymer materials: design, synthesis, and applications. *Chemical Society Reviews* **2017**, *46* (11), 3322-3356.
13. Cooper, A. I., Conjugated microporous polymers. *Advanced Materials* **2009**, *21* (12), 1291-1295.
14. Xu, Y.; Jin, S.; Xu, H.; Nagai, A.; Jiang, D., Conjugated microporous polymers: design, synthesis and application. *Chemical Society Reviews* **2013**, *42* (20), 8012-8031.

15. McKeown, N. B.; Budd, P. M., Polymers of intrinsic microporosity (PIMs): organic materials for membrane separations, heterogeneous catalysis and hydrogen storage. *Chemical Society Reviews* **2006**, *35* (8), 675-683.
16. Wang, K.; Huang, H.; Liu, D.; Wang, C.; Li, J.; Zhong, C., Covalent triazine-based frameworks with ultramicropores and high nitrogen contents for highly selective CO<sub>2</sub> capture. *Environmental science & technology* **2016**, *50* (9), 4869-4876.
17. Wang, K.; Yang, L. M.; Wang, X.; Guo, L.; Cheng, G.; Zhang, C.; Jin, S.; Tan, B.; Cooper, A., Covalent Triazine Frameworks via a Low-Temperature Polycondensation Approach. *Angewandte Chemie International Edition* **2017**, *56* (45), 14149-14153.
18. Liu, M.; Guo, L.; Jin, S.; Tan, B., Covalent triazine frameworks: synthesis and applications. *Journal of materials chemistry A* **2019**, *7* (10), 5153-5172.
19. Ben, T.; Pei, C.; Zhang, D.; Xu, J.; Deng, F.; Jing, X.; Qiu, S., Gas storage in porous aromatic frameworks (PAFs). *Energy & Environmental Science* **2011**, *4* (10), 3991-3999.
20. Wang, J.; Huang, L.; Yang, R.; Zhang, Z.; Wu, J.; Gao, Y.; Wang, Q.; O'Hare, D.; Zhong, Z., Recent advances in solid sorbents for CO<sub>2</sub> capture and new development trends. *Energy & Environmental Science* **2014**, *7* (11), 3478-3518.
21. Wang, Q.; Luo, J.; Zhong, Z.; Borgna, A., CO<sub>2</sub> capture by solid adsorbents and their applications: current status and new trends. *Energy & Environmental Science* **2011**, *4* (1), 42-55.
22. Wang, S.; Zhang, C.; Shu, Y.; Jiang, S.; Xia, Q.; Chen, L.; Jin, S.; Hussain, I.; Cooper, A. I.; Tan, B., Layered microporous polymers by solvent knitting method. *Science advances* **2017**, *3* (3), e1602610.
23. Hou, S.; Razzaque, S.; Tan, B., Effects of synthesis methodology on microporous organic hyper-cross-linked polymers with respect to structural porosity, gas uptake performance and fluorescence properties. *Polymer Chemistry* **2019**, *10* (11), 1299-1311.
24. Huang, J.; Zhu, J.; Snyder, S. A.; Morris, A. J.; Turner, S. R., Nanoporous highly crosslinked polymer networks with covalently bonded amines for CO<sub>2</sub> capture. *Polymer* **2018**, *154*, 55-61.
25. Shao, L.; Liu, M.; Sang, Y.; Huang, J., One-pot synthesis of melamine-based porous polyamides for CO<sub>2</sub> capture. *Microporous and Mesoporous Materials* **2019**, *285*, 105-111.

26. Yang, Z.; Zhang, H.; Yu, B.; Zhao, Y.; Ma, Z.; Ji, G.; Han, B.; Liu, Z., Azo-functionalized microporous organic polymers: synthesis and applications in CO<sub>2</sub> capture and conversion. *Chemical Communications* **2015**, 51 (58), 11576-11579.
27. Zhu, Y.; Zhang, W., Reversible tuning of pore size and CO<sub>2</sub> adsorption in azobenzene functionalized porous organic polymers. *Chemical Science* **2014**, 5 (12), 4957-4961.
28. Lu, J.; Zhang, J., Facile synthesis of azo-linked porous organic frameworks via reductive homocoupling for selective CO<sub>2</sub> capture. *Journal of Materials Chemistry A* **2014**, 2 (34), 13831-13834.
29. Cui, Y.; Du, J.; Liu, Y.; Yu, Y.; Wang, S.; Pang, H.; Liang, Z.; Yu, J., Design and synthesis of a multifunctional porous N-rich polymer containing s-triazine and Tröger's base for CO<sub>2</sub> adsorption, catalysis and sensing. *Polymer Chemistry* **2018**, 9 (19), 2643-2649.
30. Geng, T.; Zhu, Z.; Zhang, W.; Wang, Y., A nitrogen-rich fluorescent conjugated microporous polymer with triazine and triphenylamine units for high iodine capture and nitro aromatic compound detection. *Journal of Materials Chemistry A* **2017**, 5 (16), 7612-7617.
31. Zhu, X.; Mahurin, S. M.; An, S.-H.; Do-Thanh, C.-L.; Tian, C.; Li, Y.; Gill, L. W.; Hagaman, E. W.; Bian, Z.; Zhou, J.-H., Efficient CO<sub>2</sub> capture by a task-specific porous organic polymer bifunctionalized with carbazole and triazine groups. *Chemical Communications* **2014**, 50 (59), 7933-7936.
32. Jiang, X.; Liu, Y.; Liu, J.; Luo, Y.; Lyu, Y., Facile synthesis of porous organic polymers bifunctionalized with azo and porphyrin groups. *RSC Advances* **2015**, 5 (119), 98508-98513.
33. Hou, S.; Tan, B., Naphthyl substitution-induced fine tuning of porosity and gas uptake capacity in microporous hyper-cross-linked amine polymers. *Macromolecules* **2018**, 51 (8), 2923-2931.
34. Gargiulo, N.; Pepe, F.; Caputo, D., CO<sub>2</sub> adsorption by functionalized nanoporous materials: a review. *Journal of nanoscience and nanotechnology* **2014**, 14 (2), 1811-1822.
35. Lashaki, M. J.; Khiavi, S.; Sayari, A., Stability of amine-functionalized CO<sub>2</sub> adsorbents: a multifaceted puzzle. *Chemical Society Reviews* **2019**, 48 (12), 3320-3405.
36. Xu, X.-Y.; Chu, C.; Fu, H.; Du, X.-D.; Wang, P.; Zheng, W.; Wang, C.-C., Light-responsive UiO-66-NH<sub>2</sub>/Ag<sub>3</sub>PO<sub>4</sub> MOF-nanoparticle composites for the capture and release of sulfamethoxazole. *Chemical Engineering Journal* **2018**, 350, 436-444.

37. Knebel, A.; Sundermann, L.; Mohmeyer, A.; Strauß, I.; Friebe, S.; Behrens, P.; Caro, J. r., Azobenzene guest molecules as light-switchable CO<sub>2</sub> valves in an ultrathin UiO-67 membrane. *Chemistry of Materials* **2017**, *29* (7), 3111-3117.
38. Walton, I. M.; Cox, J. M.; Coppin, J. A.; Linderman, C. M.; Patel, D. G. D.; Benedict, J. B., Photo-responsive MOFs: light-induced switching of porous single crystals containing a photochromic diarylethene. *Chemical Communications* **2013**, *49* (73), 8012-8014.
39. Lyndon, R.; Konstas, K.; Thornton, A. W.; Seeber, A. J.; Ladewig, B. P.; Hill, M. R., Visible light-triggered capture and release of CO<sub>2</sub> from stable metal organic frameworks. *Chemistry of Materials* **2015**, *27* (23), 7882-7888.
40. Liu, F.; Fu, W.; Chen, S., Adsorption behavior and kinetics of CO<sub>2</sub> on amine-functionalized hyper-crosslinked polymer. *Journal of Applied Polymer Science* **2019**, 48479.
41. Zhao, R.; Tan, C.; Xie, Y.; Gao, C.; Liu, H.; Jiang, Y., One step synthesis of azo compounds from nitroaromatics and anilines. *Tetrahedron letters* **2011**, *52* (29), 3805-3809.
42. Wang, S.; Song, K.; Zhang, C.; Shu, Y.; Li, T.; Tan, B., A novel metalporphyrin-based microporous organic polymer with high CO<sub>2</sub> uptake and efficient chemical conversion of CO<sub>2</sub> under ambient conditions. *Journal of Materials Chemistry A* **2017**, *5* (4), 1509-1515.
43. Li, B.; Gong, R.; Wang, W.; Huang, X.; Zhang, W.; Li, H.; Hu, C.; Tan, B., A new strategy to microporous polymers: knitting rigid aromatic building blocks by external cross-linker. *Macromolecules* **2011**, *44* (8), 2410-2414.
44. İslamoğlu, T.; Rabbani, M. G.; El-Kaderi, H. M., Impact of post-synthesis modification of nanoporous organic frameworks on small gas uptake and selective CO<sub>2</sub> capture. *Journal of Materials Chemistry A* **2013**, *1* (35), 10259-10266.
45. Fayemiwo, K. A.; Vladislavljević, G. T.; Nabavi, S. A.; Benyahia, B.; Hanak, D. P.; Loponov, K. N.; Manović, V., Nitrogen-rich hyper-crosslinked polymers for low-pressure CO<sub>2</sub> capture. *Chemical Engineering Journal* **2018**, *334*, 2004-2013.
46. Xu, C.; Hedin, N., Microporous adsorbents for CO<sub>2</sub> capture—a case for microporous polymers? *Materials Today* **2014**, *17* (8), 397-403.
47. Bhunia, A.; Boldog, I.; Möller, A.; Janiak, C., Highly stable nanoporous covalent triazine-based frameworks with an adamantane core for carbon dioxide sorption and separation. *Journal of Materials Chemistry A* **2013**, *1* (47), 14990-14999.

48. Dawson, R.; Adams, D. J.; Cooper, A. I., Chemical tuning of CO<sub>2</sub> sorption in robust nanoporous organic polymers. *Chemical Science* **2011**, *2* (6), 1173-1177.
49. Patel, H. A.; Je, S. H.; Park, J.; Chen, D. P.; Jung, Y.; Yavuz, C. T.; Coskun, A., Unprecedented high-temperature CO<sub>2</sub> selectivity in N<sub>2</sub>-phobic nanoporous covalent organic polymers. *Nature communications* **2013**, *4*, 1357.
50. Raganati, F.; Alfe, M.; Gargiulo, V.; Chirone, R.; Ammendola, P., Isotherms and thermodynamics of CO<sub>2</sub> adsorption on a novel carbon-magnetite composite sorbent. *Chemical Engineering Research and Design* **2018**, *134*, 540-552.
51. Adelodun, A. A.; Ngila, J. C.; Kim, D.-G.; Jo, Y.-M., Isotherm, thermodynamic and kinetic studies of selective CO<sub>2</sub> adsorption on chemically modified carbon surfaces. *Aerosol Air Qual. Res* **2016**, *16*, 3312-3329.
52. Jing, X.; Zou, D.; Cui, P.; Ren, H.; Zhu, G., Facile synthesis of cost-effective porous aromatic materials with enhanced carbon dioxide uptake. *Journal of Materials Chemistry A* **2013**, *1* (44), 13926-13931.
53. Yuan, R.; Ren, H.; Yan, Z.; Wang, A.; Zhu, G., Robust tri (4-ethynylphenyl) amine-based porous aromatic frameworks for carbon dioxide capture. *Polymer Chemistry* **2014**, *5* (7), 2266-2272.